Systematics of the double giant dipole resonances in nuclei

J. Bar-Touv and S. Mordechai
Department of Physics, Ben-Gurion University of the Negev, P.O. Box 653, Beer-Sheva 84105, Israel
(Received 8 July 1991)

A generalization of the continuum open-shell r-space linear response random-phase approximation method to finite temperatures (i.e., TDRPA method) is applied in a study of the systematics of the electric double giant dipole resonance (DGDR) in magic and open-shell nuclei covering a wide range of nuclear masses. Viewing the DGDR as a single-phonon vibration in a hot nucleus, whose temperature corresponds to the centroid energy of the ground-state (zero-temperature) GDR, the TDRPA equation has been solved for the eleven nuclei whose DGDR state has recently been investigated in pion double-charge-exchange (DCX) experiments. The expected general features of a collective vibration in hot nuclei, particularly the broadening and the downshift of the GDR excitation energy due to increase in temperature, were found to be small, yet quite distinguishable. Except for the lighter nuclei, a reliable estimate for the DGDR energy would be $E^{\mathrm{DGDR}} \approx 2E^{\mathrm{GDR}}$ and the estimate for its width would be $\Gamma^{\mathrm{DGDR}} \approx \sqrt{2}\Gamma^{\mathrm{GDR}}$. However, the changes in the integrated cross sections of the DGDR due to finite temperature are found to be much more significant. An exact $A^{-1/6}$ power law for the DGDR energy is suggested by the TDRPA solutions. A gratifying agreement between the TDRPA predictions and experiment has been established for the Q values of the relevant pion DCX reactions after taking into account the proper Coulomb and symmetry energy corrections.

PACS number(s): 21.10.Re, 21.60.Jz, 24.30.Cz, 25.80.Hp

I. INTRODUCTION

Until recently, the investigation of giant resonances superimposed on highly excited states of a nucleus has mainly been done by deep inelastic heavy-ion nuclear collisions [1–5]. The large excitation energy dumped into the nuclear system through many degrees of freedom by the colliding heavy ions and the fast thermalization of the hot nucleus produced in the collision justify the incorporation of statistical theory considerations in interpreting the ensuing collective vibration of the hot nucleus, both experimentally and theoretically. An abrupt change in the exponentially falling curve describing the observed photon spectrum is the signature for the existence of a giant resonance vibration. The main features of electric giant dipole resonance (GDR) exposed in such experiments are a broadening of GDR as well as a downshift of its energy with increasing temperature of the hot nucleus.

The two main drawbacks of heavy-ion collision as a tool for investigating giant resonances superimposed on highly excited nuclear states are the poor selectivity of the collision process (i.e., the incapability of choosing the excited state, upon which the giant resonance is to be built) and doubt regarding the presumed global equilibration of the hot nucleus, stemming from a large background of high-energy photons as well as bremsstrahlung photons accompanying the measured γ spectrum.

A special case of selective excitation of a giant resonance in a hot nucleus is that of double giant dipole resonance (DGDR), i.e., GDR superimposed on the ground-state GDR. The possibility of exciting the DGDR and higher multidipole states has been widely discussed in recent years in several theoretical papers and experimental proposals in the context of relativistic heavy-ion collisions [6,7]. However, the first experimental verification [8] of the existence of DGDR has been achieved utilizing the highly selective reactions of pion double charge exchange (DCX). Since the DCX reactions (π^+,π^-) and (π^-,π^+) are inherently at least two-step processes in which the isotensor $(\Delta T=2,\ \Delta T_z=\pm 2)$ states are reached, it is most suited for a DGDR study since the underlying structure of that state is predominantly two-particle–two-hole (2p-2h) in nature.

The standard theoretical tool to describe DGDR is the quasiboson equation-of-motion method [9], which views DGDR as a two-phonon state, whose intrinsic structure is determined by diagonalizing the p-h residual interaction in the composite space of the 1p-1h and 2p-2h configurations. However, beside the vast numerical complications stemming from the large dimension of the 2p-2h subspace, the equation of motion for two-phonon vibrations suffers from internal defects. The coupling between the 2p-2h and 1p-1h hampers the validity of the quasiboson approximation, which is the pillar of the whole method, and extreme simplifications have to be introduced to enable a practical application of that method. An extreme schematic model based on presumed degeneracy of all 1p-1h energies has recently been applied to investigate DGDR in double-magic nuclei [10]. An SU(3) limit to the interacting boson model (IBM) has also been recently applied to DGDR states in deformed nuclei [11].

In the present study we would like to utilize an alternative viewpoint by considering DGDR plainly as a single $E1$ phonon vibration built of a coherent superposition 1p-1h excitation in a hot nucleus, whose temperature corresponds to the excitation energy of the ground-state (zero-temperature) GDR. Hence, in the framework of

the temperature-dependent random-phase approximation (TDRPA), the starting point for determining the DGDR state is the solution of the temperature-dependent Hartree-Fock (TDHF) equations, which determine the changes in the nuclear mean field with increasing temperature. The TDHF+TDRPA approach to collective motion was widely used in studying the GDR state in hot nuclei [12–16] and in interpreting the data accumulated in the last decade in deep-inelastic heavy-ion experiments. Most of those applications of the TDRPA method center on the temperature dependence of GDR in double-magic hot nuclei.

Since the first verification of the existence of the DGDR, an extensive experimental exploit of pion DCX reactions [17–21] produced an impressive amount of data on DGDR covering a wide range of the nuclear mass table. We believe that the available data are already quite sufficient to investigate the systematics of DGDR regarding its energy, width, and intergrated $E1$ total cross section. Since the available DGDR data are mainly on open-shell nuclei, it is imperative to match the TDRPA method to that particular problem. To this end we employ in the present study the most comprehensive, yet simple to apply TDRPA method [16], which constitutes a generalization of the $T=0$ r-space linear-response method of Shlomo, Bertsch, and Tsai [22,23] and the open-shell linear-response (OSLR) method of Bar-Touv and Moalem [24,25] to finite temperatures. The main ingredients added to the TDRPA method by that generalization are the inclusion of the whole continuum in the TDRPA integral equation and the possibility of the effective replacement of a complex configuration mixing of an open-shell hot nucleus by a set of fractional occupation parameters having a Fermi distribution shape. Moreover, the imposition of 1p-1h excitations on partially occupied single-particle states amounts to a straightforward coupling of the 1p-1h states to the higher-order p-h excitations, hence leading to the inclusion of part of the spreading width usually missing from a standard application of the RPA.

This paper is organized as follows: In Sec. II we present an updated summary of the results of pion DCX experiments performed recently at LAMPF. Section III is devoted to a brief outline of the TDRPA method and the manner in which it has been applied in the present study. Detailed systematics of DGDR resulting from the TDRPA theory and a comparison with experiments are the topics of Sec. IV. A summary and conclusions are given in Sec. V.

II. AN OVERVIEW ON EXPERIMENTAL RESULTS

Experiments carried out at the Los Alamos Meson Physics Facility (LAMPF) discovered the existence of two previously unobserved collective modes of the nucleus: the isotensor GDR built on the isobaric analog state (GDR⊗IAS) [17,18] and the isotensor DGDR [8,19,20,21]. A schematic representation of single giant resonances ($\Delta T=1$, $\Delta T_z=-1$) and of double giant resonances ($\Delta T=2$, $\Delta T_z=-2$) reached in pion single-charge-exchange (SCX) and pion DCX reactions is displayed in Fig. 1. The data indicate that the newly observed DGDR's are common phenomena in all nuclei and the GDR⊗IAS states are a common feature in nuclei with $N-Z\geq 1$. Figure 2 shows a typical DCX spectra from a LAMPF experiment, in which the isotensor dou-

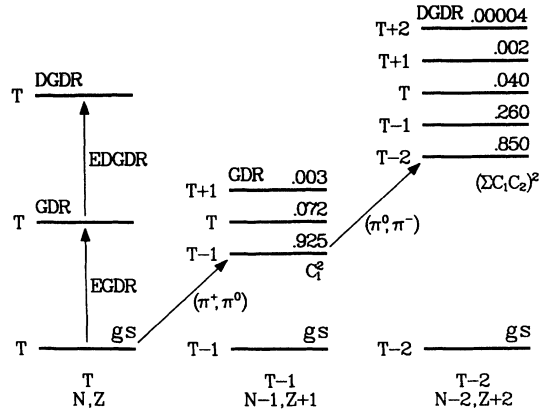

FIG. 1. Schematic energy-level diagram of the single dipole in the $\Delta T_Z=-1$ mode (GDR) and double dipole (DGDR) observable in pion single- (SCX) and double-charge-exchange (DCX) experiments, compared with double giant dipole resonance in the target nucleus ($\Delta T_Z=0$ mode) calculated using RPA and TDRPA methods. The listed numbers are the strength ratios estimated from simple isospin-coupling arguments for the case of ^{138}Ba and assuming the same reduced matrix elements for the various isospin members.

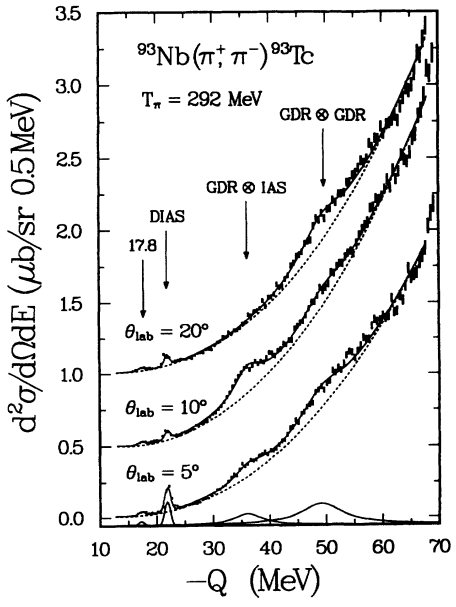

FIG. 2. Double-differential cross-section spectra measured recently at LAMPF for the (π^+,π^-) reaction of a ^{93}Nb target at $T_\pi=292$ MeV and $\theta_{lab}=5°$, 10°, and 20°. The arrows indicate the three double resonances observable in pion DCX: (1) the double isobaric analog state (DIAS), (2) the giant dipole built on the isobaric analog state (GDR⊗IAS), and (3) the double giant dipole resonance (GDR⊗GDR).

ble resonances were studied. The figure presents Q-value histograms measured for the ^{93}Nb$(\pi^+,\pi^-)^{93}$Tc reaction at 292 MeV at three different scattering angles [19]. These spectra were taken in long DCX measurements in order to accumulate good statistics. They also cover a wide range of excitation energies. The double isobaric analog state (DIAS) appears at $Q=-21.9$ MeV and is clearest in the 5° spectrum. In addition to the DIAS, two wider peaks are apparent in the spectra: the GDR⊗IAS and DGDR peaks. The first appears at $Q=-35.8$ MeV and the latter at $Q=-49.9$ MeV. The fits shown use $\Gamma_{\rm DIAS}=0.8$ MeV, $\Gamma_{\rm DGR\otimes IAS}=5.8$ MeV, and $\Gamma_{\rm DGDR}=8.8$ MeV. At 20° the GDR⊗IAS peak vanishes, but shows up clearly at 10°. DGDR has a different angular distribution. Full angular distributions for the resonances have been measures on ^{40}Ca, ^{93}Nb, and ^{50}Fe [19]. A detailed analysis shows that while the GDR⊗IAS has a dipole shape, the higher DGDR has a quadrupole distribution. Its identification as a DGDR is based on its energy (being about twice the energy of the single-step GDR), angular-distribution, and cross section.

In the following three paragraphs, we outline the main experimental features of the DGDR as they have emerged from recent DCX experiments performed at LAMPF on a wide range of masses.

(a) Energy: In (π^+,π^0) SCX data, the GDR appears at about 25 MeV. It is remarkable that the GDR energy is very weakly dependent on A [26]. This feature is due to the near cancellation of two terms: The $E1$ vibrational energy goes down with A (e.g., like $1/A^{1/3}$ or $1/A^{1/6}$); however, the Coulomb energy involved in the SCX process goes up with A, leaving the charge-exchange GDR around 25 MeV and nearly unaffected by A. The DGDR observed in pion DCX appears surprisingly close to twice the energy of the single GDR [i.e., around $Q=-50$ MeV for a wide range of masses (Table I)], as would be expected, if we neglect the isospin splitting of the double dipole, discussed later.

(b) Width: Until now the DGDR has been observed on target nuclei covering a wide range of masses (Table I). The data indicate that DGDR has a full width at half maximum (FWHM) of about 8–10 MeV and is larger than the width of the single GDR [19] by a factor of 1.5–2.0. This was found to be in a good agreement with simple theoretical estimates for the width of the double dipole in terms of two-phonon states [19,27].

(c) Cross section: It was found [19] that the peak cross section for DGDR increases by about a factor of 2 from ^{40}Ca to ^{197}Au. A qualitative argument to understand this feature was given in Ref. [19] by breaking the cross section for DGDR into a product of strength times an attenuation factor due to the distortion of the pion waves inside the nuclear medium. It was found that the 5° cross sections for DGDR in pion DCX are well represented by the function

$$\frac{d\sigma}{d\Omega}(5^\circ)_{\rm DGDR}\approx\left[\frac{NZ}{A^{2/3}}\right]^2 A^{-2.28}, \quad (1)$$

where $(NZ/A^{2/3})^2$ is the dipole transition strength deduced from the $E1$ classical sum rule, and $A^{-2.28}$ is an A-dependent attenuation factor for the incoming pions. Table I summarizes the observed quantities for DGDR in 11 nuclei ranging from ^{12}C to ^{197}Au [8,19,21]. Also listed are rough estimates for the angle-integrated cross sections extracted by normalizing distorted-wave impulse approximation (DWIA) calculations (using the code NEWCHOP [28]) to the experimental cross section at $\theta_{\rm lab}=5°$ and using the equation $\sigma_{\rm tot}=2\pi\sum\sigma(\theta_i)\sin\theta_i d\theta_i$.

III. OUTLINE OF THE CONTINUUM TDRPA METHOD AND ITS APPLICATION TO DGDR IN OPEN-SHELL NUCLEI

We hereby bring a brief outline of the generalization of the $T=0$ OSLR method [24,25] to finite temperatures. A detailed account of that generalization was given in Ref. [16].

In the context of the HF-RPA approximation, the OSLR method is designed to take into account a possible

TABLE I. Systematics of double isovector giant dipole resonance from pion double-charge-exchange experiments at LAMPF.

Target nucleus	Q (DGDR) (MeV)	Γ (DGDR) (MeV)	$d\sigma/d\Omega$ (DGDR) (μb/sr)	$\sigma_{\rm tot}$ (DGDR)[a] (μb)	Ref.
^{12}C	−48.2±2.0	10.0±3.0	0.86±0.18	6.7	[19]
^{13}C	−46.5±2.0	12.0±3.0	3.20±0.53	25.2	[19]
^{27}Al	−49.1±0.5	8.4±2.0	2.41±0.23	18.6	[20]
^{32}S	−49.6±2.0	9.0±2.0	0.98±0.31	5.0	[8,19]
^{40}Ca	−54.0±0.5	9.0±1.4	2.6±0.2	12.9	[20]
^{56}Fe	−54.4±0.6	10.0±1.5	3.12±0.31	15.2	[19]
^{59}Co	−48.6±0.8	8.2±2.0	4.05±0.75	19.7	[19]
^{93}Nb	−49.9±0.8	8.8±2.6	3.48±0.47	17.8	[19]
^{115}In[b]	−49.1±2.0	8.0±2.0	12.4±3.7	66.3	
^{138}Ba	−49.8±0.8	8.5±2.6	4.2±0.5	23.6	[19]
^{197}Au	−52.1±0.8	10.0±2.0	5.7±2.0	41.2	[19]

[a]Angle-integrated cross section for the double dipole obtained by normalizing the DWIA calculations to the experimental peak cross section at $\theta_{\rm lab}=5°$. $\sigma_{\rm tot}=2\pi\sum\sigma(\theta_i)\sin\theta_i d\theta_i$.

[b]Preliminary results.

complex configuration mixing in the ground-state wave function in a straightforward manner, while calculating the excited states of a nucleus. The two main ingredients of the OSLR method are as follows: (i) The excited states of a nucleus are related to the poles of the RPA Green's function [22,23]

$$G^{\mathrm{RPA}}=G^{(0)}\left[1-G^{(0)}\frac{\partial V}{\partial\rho}\right]^{-1}, \tag{2}$$

where $G^{(0)}$ is the unperturbed Green's function and $\partial V/\partial\rho$ is the derivative of the HF mean-field potential with respect to the HF nuclear density. (ii) A set of single-particle occupation parameters can effectively represent a possibly complex configuration mixing in a correlated ground-state wave function. The contractions made in linearizing the RPA equations are thus performed with a single-determinant wave composed of fully and partially occupied single-particle orbitals. Assuming that the main properties of DGDR (energy, width, and $E1$ strength distribution) are practically independent of the particular value of the ground-state angular momentum and isospin, the 1p-1h excitations leading to the collective dipole vibration may be superimposed on the HF intrinsic determinant without projecting the total angular momentum or isospin. Obviously, this conjecture would be justified *a posteriori* by the predictions of the model discussed later. Hence the simplicity of the uncoupled spherical m scheme is preserved in all the states of the HF and RPA calculations.

The two aforementioned conjectures are combined into a modified unperturbed Green's function [16],

$$G^{(0)}(r,r',E)=-\sum\theta_{\mathrm{h}}\phi_{\mathrm{h}}^{*}(r)[g(r,r',\varepsilon_{\mathrm{h}}+E)+g(r,r',\varepsilon_{\mathrm{h}}-E)]\phi_{\mathrm{h}}(r')+\Delta\ , \tag{3}$$

where θ_{h} is the occupation parameter for a hole state and g is the single-particle Green's function obeying the proper boundary conditions for all energies (negative and positive). Δ is a Pauli correction term included to avoid double counting of p-h excitations among the partially occupied states.

The temperature dependence is readily propagated through the HF mean field and RPA equation by utilizing a Fermi distribution to represent the occupation parameters $\theta_j(T)$, i.e.,

$$\theta_j(T)=\{1+\exp[(\varepsilon_j-\mu)/kT]\}^{-1}\ . \tag{4}$$

ε_j is the single-particle energy of the temperature-dependent HF (TDHF) field and μ is the chemical potential serving as a Lagrange multiplier for the number of particle constraints. The generalization of the RPA equation [Eq. (2)] into a TDRPA equation is readily achieved by expressing the unperturbed Green's function of Eq. (3) in terms of the predetermined TDHF single-particle basis and occupation parameters. Temperature dependence is also carried to the residual p-h interaction by identifying $V_{\text{p-h}}$ as the derivative of the TDHF potential with respect to the temperature-dependent nuclear density.

Once the temperature-dependent $G^{(0)}$ and G^{RPA} are determined, the response of the nucleus to an external field represented by the single-particle operator F is determined by [22]

$$R_F(E,t)=\langle FG^{\mathrm{RPA}}F\rangle=\int dr_1dr_2F(r_1)F(r_2)G(r_1,r_2,E,T)\ , \tag{5}$$

and the transition strength by

$$S_F(E,t)=-\frac{1}{\pi}\,\mathrm{Im}\langle FG^{\mathrm{RPA}}F\rangle\ . \tag{6}$$

IV. APPLICATION OF THE TDRPA METHOD TO DGDR IN MAGIC AND OPEN-SHELL NUCLEI

The search for DGDR in a particular nucleus begins with a proper choice for the trial ground-state configuration to be used in solving the HF ($T=0$) equations. For all 11 nuclei investigated in the present study (Table I), we have taken the simplest shell-model ground-state configuration [29]; e.g., $^{93}_{52}\mathrm{Nb}_{41}$ taken as

$$|^{93}_{52}\mathrm{Nb}_{41}\rangle=|^{90}_{50}\mathrm{Zr}_{40}\rangle|2d^{2}_{5/2}\rangle_n|1g_{9/2}\rangle_p\ , \tag{7}$$

with the corresponding open-shell single-particle occupation parameters $\theta_n(2d_{5/2})=\frac{1}{3}$ and $\theta_p(1g_{9/2})=\frac{1}{10}$. With such predetermined occupation parameters, the HF mean field and ensuing GDR are calculated using a zero-range Skyrme I (SKI) force [30]. The same set of occupation parameters is used as a starting point for the TDHF solution, ending with the dispersion of occupation into a larger set of single-particle levels around the Fermi surface. The TDHF solution, whose total energy equals the energy of the RPA ground-state single GDR, is used in solving the TDRPA equation [Eq. (2)]. As mentioned above, the DGDR state is considered as single GDR superimposed on that finite-temperature HF solution.

In deriving the p-h interaction $V_{\text{p-h}}$ with the aid of Landau's prescription (i.e., $V_{\text{p-h}}=\partial V_{\mathrm{HF}}/\partial\rho_{\mathrm{HF}}$), we employ for simplicity the total nuclear density $\rho(r)=\rho_n(r)+\rho_p(r)$ and an average field

$$V_{\mathrm{HF}}(r)=\frac{Z}{A}V_p(r)+\frac{N}{A}V_n(r)\ , \tag{8}$$

where ρ_p, V_p, ρ_n, and V_n are the calculated HF and TDHF proton and neutron densities and potentials. We also replaced the Laplacians entering the p-h interaction $V_{\text{p-h}}$ with the approximate expression

$$k^2=\left[\frac{2m^{*}(r)}{h^2}\right][E_{\mathrm{HF}}/A-V_{\mathrm{HF}}(r)]\ . \tag{9}$$

Using this approximation and the interaction strength coefficients determined by Tsai [31] for each of the four spin-isospin components of the p-h interaction

$$V_{\text{p-h}}=\delta(r_{12})(F_0+F_0'\tau\cdot\tau+G_0\sigma\cdot\sigma+G_0'\sigma\cdot\sigma\tau\cdot\tau)\ , \tag{10}$$

we arrive at the following expressions:

$$v_{\text{p-h}}(S=0,T=0)=\tfrac{3}{4}t_0+\tfrac{3}{8}t_3\rho+\tfrac{1}{8}k^2(3t_1+5t_2)\ , \tag{11a}$$

$$V_{\text{p-h}}(S=0,T=1) = -\tfrac{1}{4}t_0(1+2x_0)-\tfrac{1}{8}t_3\rho-\tfrac{1}{8}k^2(t_1-t_2)\ , \quad (11b)$$

$$V_{\text{p-h}}(S=1,T=0) = -\tfrac{1}{4}t_0(1-2x_0)-\tfrac{1}{8}t_3\rho-\tfrac{1}{8}k^2(t_1-t_2)\ , \quad (11c)$$

$$V_{\text{p-h}}(S=1,T=1) = -\tfrac{1}{4}t_0-\tfrac{1}{8}t_3\rho-\tfrac{1}{8}k^2(t_1-t_2)\ . \quad (11d)$$

The preference of SKI force parameters t_0, t_1, t_2, t_3, and x_0 in the present study is quite arbitrary. No effort has been done to choose among the available different sets of Skyrme force parameters in order to gain a best fit to experiment.

Table II summarizes the predictions of the RPA and TDRPA methods in the manner that they have been applied in the present study. The table also includes the experimental single GDR energies, integrated $E1$ cross sections, and widths measured mainly in photonuclear reactions [32,33]. Considering the aforementioned approximations used in applying the TDRPA method, a measure of confidence in the theoretical prediction of that model for the main features of DGDR is suggested by the remarkably satisfactory agreement of the calculated single GDR energies, widths, and integrated $E1$ cross sections with the photonuclear data. An $A^{-1/6}$ power-law least-squares fit for the 11 calculated ground-state GDR energies leads to the relation

$$E^{\text{GDR}}_{\text{RPA}} = (34.4\pm0.5)A^{-1/6}\ \text{MeV}\ , \quad (12)$$

while the corresponding fit for the experimental GDR energies gives a very close relation

$$E^{\text{GDR}}_{\text{expt}} = (33.5\pm0.4)A^{-1/6}\ \text{MeV}\ . \quad (13)$$

Hence the systematics of the DGDR energies as predicted by the TDRPA method obey the $A^{-1/6}$ power law

$$E^{\text{DGDR}}_{\text{TDRPA}} = (33.5\pm0.4)A^{-1/6}\ \text{MeV}\ . \quad (14)$$

A comparison between the theoretical predictions for $E^{\text{GDR}}_{\text{RPA}}$ and $E^{\text{DGDR}}_{\text{TDRPA}}$ [Eqs. (12) and (14)] reveals a small downshift in the DGDR energy due to the finite temperature of the TDHF mean field, upon which the DGDR state is superimposed. A similar shift in the GDR energy with increasing temperature was previously observed in deep-inelastic heavy-ion experiments [1–5] and supported by other RPA calculations in hot nuclei [12–16]. Yet, considering the relatively high temperature ($T=3.4$ MeV in ^{12}C and $T=1.05$ MeV in ^{191}Au) needed to produce a TDHF mean field whose excitation energy matches that of the ground-state ($T=0$) GDR, the temperature effects of E^{DGDR} are rather small. Thus a good estimate for the measured DGDR energy would be $E^{\text{DGDR}}\approx 2E^{\text{GDR}}$.

A two-parameter least-squares fit aiming to a power law for the giant resonances energies, in which the strength and exponent are free to vary, leads to the relations

$$E^{\text{GDR}}_{\text{RPA}} = 40.3A^{-0.206}\ \text{MeV}\ , \quad (15a)$$

$$E^{\text{GDR}}_{\text{expt}} = 38.3A^{-0.188}\ \text{MeV}\ , \quad (15b)$$

$$E^{\text{DGDR}}_{\text{TDRPA}} = 33.8A^{-0.169}\ \text{MeV}\ . \quad (15c)$$

The calculated $E^{\text{DGDR}}_{\text{TDRPA}}$ seem to obey exactly the $A^{-1/6}$ law predicted by the macroscopic two-fluid model for GDR [34] based on a presumed $A^{-1/6}$ dependence of the restoring force of the collective motion on the nuclear surface area. Figure 3 displays the above power laws of the two-parameter least-squares fits.

Turning now to the calculated integrated cross sections for GDR and DGDR (Table II), we note some differences between the two. Part of the difference in σ_{int} may be attributed to the superiority of the TDHF ground-state wave function over the simple shell-model configuration used in solving the $T=0$ HF equations, since the finite-temperature mean field is free to choose its own single-particle occupation parameters $\theta_j(T)$, while those of the $T=0$ mean field are predetermined. A second source for the difference in σ_{int} lies in the velocity-dependent com-

TABLE II. RPA and TDRPA predictions for GDR and DGDR in the nuclei investigated in pion DCX reactions (see Table I). The photonuclear data on the ground-state GDR's are taken from Refs. [32] and [33] and references therein.

	GDR (RPA)					DGDR (TDRPA)					GDR (photo)				
A	E (MeV)	Γ^{a} (MeV)	σ_{int} (mb MeV)	SRF[b] (%)	$EA^{1/6}$ (MeV)	E (MeV)	Γ^{a} (MeV)	σ_{int} (mb MeV)	SRF (%)	$EA^{1/6}$ (MeV)	E (MeV)	Γ^{c} (MeV)	σ_{int} (mb MeV)	SRF (%)	$EA^{1/6}$ (MeV)
^{12}C	24.2	9.6	142	79	36.6	21.1	12.7	139	78	31.9	23.0	~7.0	150	83	34.8
^{13}C	22.7	12.6	166	86	34.8	21.0	12.2	158	82	32.2	23.8				36.5
^{27}Al	21.1	7.2	393	97	36.7	19.8	8.3	362	90	34.4	21.4	~7.5	400	99	37.1
^{32}S	19.1	7.1	401	83	34.0	19.3	6.9	423	88	34.4	19.6	~7.5	460	96	34.9
^{40}Ca	18.8	6.5	580	97	34.8	18.8	6.8	508	85	34.8	19.9	~6.4	642	107	36.8
^{56}Fe	18.0	5.5	931	111	35.2	17.7	5.5	818	98	34.6	17.6				34.4
^{59}Co	17.7	5.0	966	110	34.9	17.7	5.0	847	96	34.9	18.0	~6.2	884	101	35.5
^{93}Nb	15.8	4.1	1372	100	33.6	16.1	5.1	1002	73	34.3	16.6	5.1	1331	97	35.3
^{115}In	15.1	3.8	1741	103	33.3	14.6	5.0	1722	102	32.2	15.6	4.9	1875	111	34.4
^{138}Ba	14.4	4.8	1934	97	32.7	14.8	4.7	1569	79	33.6	15.3	4.9	2190	102	34.8
^{197}Au	13.1	5.3	2907	102	31.6	12.9	4.9	2707	89	31.1	13.8	4.1	2967	105	33.3

[a]Estimated by convolution of a single Gaussian distribution to the calculated $E1$ cross sections [Eq. (16)].
[b]Sum rule fraction (SRF) $= \sigma_{\text{int}}/(60NZ/A)$.
[c]Estimates from experimental $E1$ cross sections and by Lorentzian fits to experiments [32].

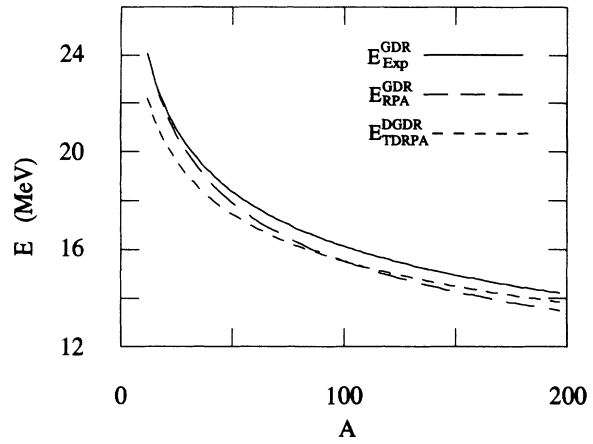

FIG. 3. Systematics of GDR and DGDR energies as functions of mass number A. The three curves represent the power laws [Eqs. 15(a), 15(b), and 15(c)] obtained by two-parameter least-squares fits to the calculated E^{GDR}_{RPA} and E^{DGDR}_{TDRPA} and to photonuclear data for the isovector GDR. The data points for these fits are those listed in Table II.

ponents included in the SKI $V_{p\text{-}h}$ interaction (affected by the parameters t_1 and t_2). In the absence of such a component in $V_{p\text{-}h}$, one expects σ_{int} to be independent of temperature [14]. In Fig. 4 we plot the calculated cross sections versus energy for GDR and DGDR in ^{12}C. To demonstrate more conspicuously the changes in the DGDR due to an increase in temperature, we have backshifted in the figure the DGDR downward by 24.1 MeV to coincide with the centroid energy of ground-state ($T=0$) GDR. Beside the small shift in the $E1$ cross section, we note an enhancement of $E1$ strength just below the main peak of the GDR together with an expected decrease in $E1$ threshold. A significant overall reduction in

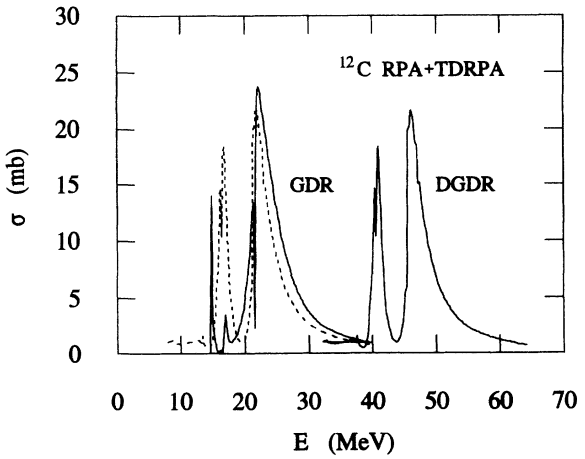

FIG. 4. GDR and DGDR $E1$ cross sections obtained from RPA and TDRPA solutions in ^{12}C. The dashed curve is identical to that of DGDR, backshifted by 24.1 MeV to eliminate its energy elevation as a GDR built on the ground-state GDR. This backshift is done in order to stress the finite-temperature effects on a GDR state in hot nuclei.

the integrated cross sections of the DGDR state is also noticed, particularly for the lighter nuclei.

The calculated widths given in Table II are qualitative estimates for the widths of the GDR and DGDR states derived by matching a single Gaussian distribution to the calculated strength distribution $S_F(E,T)$ of Eq. (6). A normal distribution would include 76% of the strength in the energy range $(-\Gamma/2,\Gamma/2)$. Hence cutting 12% of the $E1$ integrated strengths on the lower and upper tails of the corresponding curve determines the Gaussian estimate for Γ. As for the true width of the DGDR state to be compared with experiment, we still have to take a convolution of the single and double resonances if we assume that the excitation of the two corresponds to statistically independent processes. Hence the theoretical estimate for the total width of the DGDR state denoted by Γ_{theor} is determined by

$$\Gamma_{theor}=[(\Gamma^{GDR}_{RPA})^2+(\Gamma^{DGDR}_{TDRPA})^2]^{1/2}\ , \tag{16}$$

where Γ^{GDR}_{RPA} and Γ^{DGDR}_{TDRPA} are the individual widths of the two states. Such a qualitative estimate for widths is expected to be quite reliable for a comparative study of temperature and mass effects on the giant resonance. Except for ^{12}C, all the theoretical widths Γ_{theor} fall in the energy range determined in the corresponding pion DCX experiment. Since the individual widths Γ^{GDR}_{RPA} and Γ^{DGDR}_{TDRPA} are roughly equal (except for the lighter nuclei), a reliable estimate for the DGDR width would be $\Gamma^{DGDR}_{TDRPA}\approx\sqrt{2}\Gamma^{GDR}_{RPA}$.

We conclude the present survey of our results in a comparison of the TDRPA predictions for E^{DGDR} with the energies measured in pion DCX experiments. In doing so, we should recall that the DGDR studied in the framework of TDRPA theory is a double resonance in the target nucleus itself (i.e., $\Delta T_z=0$), while a DGDR reached in pion DCX reactions is a double resonance in a neighbouring $\Delta T_x=-2$ nucleus. Hence we must take into account a two-step Coulomb energy correction and the isospin splitting of the DGDR. The Coulomb energy correction for the successive transfer of two charges is determined by the empirical relations [35,36]

$$\Delta E_{C1}=1.44(Z+\tfrac{1}{2})A^{-1/3}-1.13\ \text{MeV} \tag{17a}$$

and

$$\Delta E_{C2}=1.44(Z+\tfrac{3}{2})A^{-1/3}-1.13\ \text{MeV}\ . \tag{17b}$$

Here Z and A are the charge and mass numbers of the target nucleus. The combined energy correction due to the double charge exchange is determined by

$$E^{sum}=E^{GDR}_{RPA}+E^{DGDR}_{TDRPA}+(\Delta E_{C1}-\delta)+(\Delta E_{C2}-\delta)\ , \tag{18}$$

where $\delta=M_n-M_p=1.29$ MeV. As for the symmetry energy corrections, a simple double-isospin-coupling argument [35] (assuming all five isospin components of the $\Delta T=2$ reaction have the same matrix elements) suggests that the lowest isospin state (the $T-2$ member of the quintet) is by far the dominant state in nuclei with $A>93$ (Fig. 1). Hence the energy shift in the DCX reaction due to isospin splitting may be reliably estimated by

TABLE III. Reconstruction of the RPA and TDRPA predictions for the double giant dipole resonance Q values.

Target	E_{RPA}^{GDR} (MeV)	E_{TDRPA}^{DGDR} (MeV)	$(\Delta E_{C1}-\delta)$[a] (MeV)	$(\Delta E_{C2}-\delta)$[b] (MeV)	E^{sum}[c] (MeV)	ΔE^{-}[d] (MeV)	ΔE^{+}[d] (MeV)	$\lvert Q(\text{DGDR})\rvert$[e] (MeV)
^{12}C	24.2	21.1	1.66	2.29	49.3			49.3
^{13}C	22.7	21.0	1.56	2.17	47.4			47.4
^{27}Al	21.1	19.8	4.06	4.54	49.5			49.5
^{32}S	19.1	19.3	5.06	5.52	49.0			49.0
^{40}Ca	18.7	18.5	6.21	6.63	50.0			54.0
^{56}Fe	17.8	17.5	7.55	7.75	50.6	1.8	2.7	50.6
^{59}Co	17.7	17.4	8.49	8.86	52.5	2.1	2.9	49.6
^{93}Nb	15.8	16.1	10.77	11.09	53.9	2.7	3.2	50.7
^{115}In	15.1	14.6	12.09	12.53	54.3	3.2	3.6	47.5
^{138}Ba	14.4	14.8	13.32	13.60	56.1	3.6	3.9	48.6
^{197}Au	13.1	12.9	17.26	17.50	60.76	2.5	2.6	55.7

[a]Equation (17a) and Refs. [35] and [36].
[b]Equation (17b) and Refs. [35] and [36]. Here Z is the target Z number and $\delta=m_n-m_p=1.29$ MeV.
[c]Equation (18).
[d]Equations (19a) and (19b) and Ref. [37]. $E_v=50/A$ MeV and $E_t=-0.003$ MeV.
[e]For $A>93$ the theoretical Q values are corrected for Coulomb and symmetry-energy shifts according to Eq. (20). For ^{59}Co and ^{93}Nb, Q(theory) is taken as $E^{sum}-\Delta E^{+}$.

the two shifts of the SCX reaction determined by [27]

$$\Delta E^{-}=E_T-E_{T-1}=T[E_v+(2T+3)E_t] \tag{19a}$$

and

$$\Delta E^{+}=E_{T+1}-E_T=\Delta E^{-}(T+1)/T\ , \tag{19b}$$

with the isovector energy $E_v=50/A$ MeV and the isotensor energy $E_t=-0.003$ MeV. Obviously, no-isospin splitting should be considered in nuclei of the $T=0$ ground state. In the intermediate nuclei ^{59}Co and ^{93}Nb, because of a more even partition of the excitation probability, we include only the ΔE^{+} energy shift. Subtracting the isospin energy shift from the energy sum of Eq. (18) leads to the following expression for the TDRPA prediction for the Q value of a DCX reaction:

$$Q(\text{theory})=E^{sum}-(\Delta E^{-}+\Delta E^{+})\ . \tag{20}$$

Tables III and IV summarize the calculated E_{RPA}^{GDR} and E_{TDRPA}^{DGDR} of Table II together with the corresponding aforementioned energy corrections. The resulting theoretical and experimental Q values for each of the 11 nuclei investigated in the present study are compared in Table IV. The agreement between the TDRPA Q values and the pion DCX reaction data is truly gratifying.

V. CONCLUSIONS

We have demonstrated above that the generalization of the r-space linear-response RPA to finite temperature (i.e., TDRPA) offers a most powerful method to investigate DGDR collective vibrations in magic as well as open-shell nuclei. The vast practical complexities of the alternative approach to DGDR suggested by the two-phonon equation of motion method are simply avoided by viewing the DGDR vibration as a single-phonon GDR state in a hot nucleus, whose temperature corresponds to the excitation energy of ground-state ($T=0$) GDR. A most sophisticated method, yet simple to apply, is obtained by incorporating into a single framework the TDHF and continuum TDRPA methods. A spherical m-scheme TDHF single-determinant wave function composed of fully and partially occupied orbitals opens the possibility of investigating DGDR in magic and open-shell nuclei.

The availability of enough data on the DGDR state resulting from pion DCX experiments of recent years (Table I) enabled us to put to a stringent test the TDHF+TDRPA approach to DGDR collective vibrations in a wide range of nuclear masses. The systematics

TABLE IV. Comparison between experimental and theoretical predictions for the double giant dipole resonance Q values and widths.

Target	DGDR (TDRPA)[a] $-Q$ (MeV)	DGDR (TDRPA)[a] Γ[c] (MeV)	DGDR (Expt.)[b] $-Q$ (MeV)	DGDR (Expt.)[b] Γ (MeV)
^{12}C	49.3	15.9	48.2±2.0	10.0±3.0
^{13}C	47.4	17.5	46.5±2.0	12.0±3.0
^{27}Al	49.5	11.0	49.1±0.5	8.4±2.0
^{32}S	49.0	9.9	49.6±2.0	9.0±2.0
^{40}Ca	54.0	9.4	54.0±0.5	9.0±1.4
^{56}Fe	50.6	9.5	54.4±0.6	10.0±1.5
^{59}Co	49.6	7.1	48.6±0.8	8.2±2.0
^{93}Nb	50.7	6.5	49.9±0.8	8.8±2.6
^{115}In	47.5	6.3	49.1±2.0	8.0±2.0
^{138}Ba	48.6	6.7	49.8±0.8	8.5±2.6
^{197}Au	55.7	7.2	52.1±0.8	10.0±2.0

[a]From Table III.
[b]From Table I.
[c]$\Gamma=[(\Gamma_{RPA}^{GDR})^2+(\Gamma_{TDRPA}^{DGDR})^2]^{1/2}$.

in the DGDR energies, integrated $E1$ cross section, and widths was studied for the 11 nuclei, whose DGDR state was observed in pion DCX experiments (Table II).

The expected general features of a collective vibration in hot nuclei, particularly the broadening and the downshift of the GDR excitation energy due to increase in temperature, were found to be small, yet quite distinguishable. Except for the lighter nuclei, a reliable estimate for the DGDR energy would be $E^{\mathrm{DGDR}}_{\mathrm{TDRPA}} \approx 2E^{\mathrm{GDR}}_{\mathrm{RPA}}$ and the estimate for its width would be $\Gamma^{\mathrm{DGDR}}_{\mathrm{TDRPA}} \approx \sqrt{2}\Gamma^{\mathrm{GDR}}_{\mathrm{RPA}}$ (see Table IV). However, the differences in the integrated cross sections of the DGDR due to finite temperature are found to be much more significant. The TDRPA predictions for the DGDR energy systematics suggest an exact $A^{-1/6}$ power law [Fig. 4 and Eq. (15c)] compatible with the old predictions of the two-fluid approach to GDR based on the concept of a restoring force being proportional to the nuclear surface area. A most gratifying agreement between the TDRPA predictions and experiment was established for the Q values of the relevant DCX reactions after taking into account acceptable estimates for a two-step charge-exchange Coulomb energy shift and a symmetry-energy correction stemming from the isospin splitting of the DGDR state (Tables III and IV).

ACKNOWLEDGMENTS

One of us (J.B.) wishes to thank Professor S. A. Moszkowski and other colleagues at the UCLA Physics Department for their kind hospitality. This work is supported by the U.S.–Israel Binational Science Foundation.

[1] J. O Newton *et al.*, Phys. Rev. Lett. **46**, 1383 (1981).
[2] J. E. Draper *et al.*, Phys. Rev. Lett **49**, 434 (1982).
[3] J. J. Gaardhoje *et al.*, Nucl. Phys. **A396**, 329 (1983); J. J. Gaardhoje, *ibid.* **A488**, 261c (1988).
[4] K. A. Snover, Nucl. Phys. **A482**, 13c (1988).
[5] A. M. Sandorfi *et al.*, Phys. Lett. **130B**, 19 (1983).
[6] G. Baur and C. A. Bertulani, in *The Response of Nuclei Under Extreme Conditions,* edited by R. A. Broglia and G. F. Bertsch (Plenum, New York, 1988).
[7] P. Braun-Nunziger *et al.*, Proposal 814, Alternating Gradient Synchrotron, Brookhaven, NY (unpublished).
[8] S. Mordechai *et al.*, Phys. Rev. Lett. **61**, 531 (1988)
[9] D. J. Rowe, Rev. Mod. Phys. **40**, 153 (1968).
[10] G. Lauritsch and P. G. Reinhard, Nucl. Phys. **A509**, 287 (1990).
[11] F. J. Scholtz and F. J. Hahne, Z. Phys. A **336**, 145 (1990).
[12] P. Ring *et al.*, Nucl. Phys. **A419**, 261 (1984).
[13] D. Vautherin and N. Vinh-Mau, Nucl. Phys. **A422**, 140 (1984).
[14] O. Civitarese, R. A. Broglia, and C. Dasso, Ann. Phys. (N.Y.) **156**, 142 (1984).
[15] H. Sagawa and G. F. Bertsch, Phys. Lett. **146B**, 138 (1984).
[16] J. Bar-Touv, Phys. Rev. C **32**, 1369 (1985).
[17] S. Mordechai *et al.*, Phys. Rev. Lett. **60**, 408 (1988).
[18] S. Mordechai *et al.*, Phys. Rev. C **40**, 850 (1989).
[19] S. Mordechai *et al.*, Phys. Rev. C **41**, 202 (1990).
[20] S. Mordechai *et al.*, Phys. Rev. C **43**, 1509 (1991).
[21] S. Mordechai and C. F. Moore, Nature **352**, 393 (1991).
[22] G. Bertsch and S. F. Tsai, Phys. Rep. C **18**, 125 (1975).
[23] S. Shlomo and G. Bertsch, Nucl. Phys. **A243**, 507 (1975).
[24] J. Bar-Touv, A. Moalem, and S. Shlomo, Nucl. Phys. **A339**, 303 (1980).
[25] J. Bar-Touv and A. Moalem, Nucl. Phys. **A351**, 285 (1981).
[26] A. Erell *et al.*, Phys. Rev. C **34**, 1822 (1986).
[27] N. Auerbach, A. Klein, and N. V. Giai, Phys. Lett. **106B**, 347 (1981); N. Auerbach, Ann. Phys. (N.Y.) **197**, 376 (1990).
[28] E. Rost, computer code CHOPIN (unpublished). The code has been modified by C. L. Morris to calculate pion charge-exchange reactions and renamed NEWCHOP.
[29] J. P. Elliott and A. M. Lane, in *Handbuch der Physics,* edited by S. Flügge (Springer-Verlag, Berlin, 1957), Vol. XXIX, Table 6, pp. 265–268.
[30] D. Vautherin and D. M. Brink, Phys. Rev. C **5**, 39 (1972).
[31] S. Tsai, Phys. Rev. C **17**, 1862 (1978).
[32] B. L. Berman and S. C. Fultz, Rev. Mod. Phys. **47**, 713 (1975), and references therein.
[33] J. M. Wycoff, B. Ziegler, H. W. Koch, and R. Vhlig, Phys. Rev. **137**, B576 (1964), and references therein.
[34] M. Goldhaber and E. Teller, Phys. Rev. **74**, 1046 (1948).
[35] J. D. Anderson, C. Wong, and J. W. McClure, Phys. Rev. **138**, B615 (1965).
[36] M. S. Antony, J. Britz, J. B. Buch, and A. Pape, At. Data Nucl. Data Tables **33**, 447 (1985).